ARCHIVES OF ACOUSTICS
**34**, 1, 63–74 (2009)

# Nonlinearly Coded Signals for Harmonic Imaging

Andrzej NOWICKI, Janusz WÓJCIK, Tamara KUJAWSKA

*Ultrasound Department*
*Institute of Fundamental Technological Research*
*Polish Academy of Sciences*
Świętokrzyska 21, 00-049 Warszawa, Poland
e-mail: tkujaw@ippt.gov.pl

(*received March 4, 2008; accepted October 16, 2008*)

In this paper a new method utilizing nonlinear properties of tissues to improve contrast-to-noise ratio is presented. In our novel method the focused circular transducer is excited with two-tone bursts (including the 2.2 MHz fundamental and 4.4 MHz second harmonic frequencies) with specially coded polarization of each tone. This new approach was named Multitone Nonlinear Coding (MNC) because the choice of both tones polarization and amplitude law, allowing optimization of the probe receiving properties, depends on nonlinear properties of tissue. The numerical simulations of nonlinear fields in water and in tissue-like medium with absorption coefficient of 7 Np/(m·MHz) are performed. The comparison between the proposed method and the Pulse Inverse (PI) method is presented. The concept of the virtual fields was introduced to explain properties of both the Pulse Inversion and MNC methods and to compare their abilities. It was shown that for the same on-source pressure an application of the MNC method allows to decrease the mechanical index about 40%, to improve lateral resolution from 10 to 30% and to gain the signal-to-noise ratio up to 8 times with respect to the PI method.

**Keywords:** harmonic imaging, ultrasonography, nonlinear propagation.

## 1. Introduction

Tissue Harmonic Imaging (THI) technique, described for the first time by Averkiou *et al.* [1] in 1997, nowadays is used commonly in clinical practice proving its importance in improved quality of grey-scale images, especially in examining of the, so called, "hard to image" patients [3, 4]. However, it has to be stressed that it is far from optimal in the sense that only half of the available transducer bandwidth is used for image formation – lower half for transmission and upper half during reception. The importance of both the reduced dynamic range and penetration encountered in THI was also pointed out [1, 2].

Since the images in THI technique are formed by the second or higher harmonic components, which level is usually at least 20 dB lower than the fundamental, the dynamic and penetration ranges are limited. The nonlinear effects, including contrast agents improving the imaging sensitivity was intensively studied by many authors [5–8]. An improved resolution and contrast to noise ratio can be achieved with an imaging method called Pulse Inversion (PI). In contrast to the conventional harmonic imaging, for Pulse Inversion imaging the whole frequency spectrum can be used during reception. PI method involves transmitting alternately two single-tone bursts along each scan line with the second (negative) pulse being the inverted copy of the first (positive) pulse [9]. The echoes received are then added together to build up the final scan line. Due to the nonlinear nature of wave propagation the spectra of the positive and negative pulses are not the same. For the sum signal the second harmonic is enhanced while the fundamental frequency component is reduced. This method removes the requirement of narrow band transmitting for the harmonic signal extraction and even in the case of broadband transmitting, when fundamental and harmonic components are overlapping, the harmonic component can be extracted. An extension of the PI method was reported by Toshiba as a new modality called Differential Tissue Harmonic Imaging, where transducer transmits pulses with the frequency concentrated around the fundamental and the second harmonic and pairs of transmitted pulses are shifted in phase by 180° (US Patent 2005).

The proposed novel method, named the Multitone Nonlinear Coding (MNC), involves transmitting along each scan line alternately two configurations of the two-tone bursts (including the fundamental $f_1$ and the second harmonic $2f_1$ frequencies) with specially coded polarization. During reception the addition or subtraction of the resultant echoes follows. Utilizing of the nonlinear acoustic properties of tissues the novel method can improve the ultrasonic imaging resolution and signal-to-noise ratio for the mechanical index (MI) lower than for the PI method.

The paper is organized as following. First, the basics for the nonlinear model of wave propagation in tissue are addressed. Then, a brief description of the Pulse Inversion (PI) method is given. Next, theoretical description of our novel approach, including pulses construction follows. The spectral behavior on two-tone pulses propagating in tissue are analyzed that helps to gain more insight into the various combinations of the received echoes. Afterwards, introduction of the virtual fields is presented. The concept of the virtual fields, computed out of the data acquired from the propagation of two-tone pulses, helps to explain the basic properties of the new method and to compare it to the PI method. Finally, the numerically simulated pressure incident fields for both the MNC and PI methods are discussed. It was shown that the improvement of the contrast to noise ratio without increasing the mechanical index MI is feasible with our new, MNC method.

## 2. Numerical model and boundary conditions

The model used for both the PI and MNC methods is the second-order nonlinear partial differential equation reported in [10]. The model equation describing the nonlinear distortion of the acoustic finite-amplitude wave propagating in the nonlinear dissipative medium accounts for the effects of diffraction, attenuation and nonlinearity. It was solved using the incremental steps scheme to propagate the wave forward in small steps. In the dimensionless system of variables this equation has a form:

$$\begin{gathered}\Delta P - \partial_{tt} P - 2\partial_t \mathbf{A}\, P = -q\beta\partial_{tt}\left(P\right)^2, \\ \mathbf{A}\, P \equiv A(t) \otimes P\left(\mathbf{x}, t\right), \qquad A(t) = F^{-1}\left[a(m)\right],\end{gathered} \tag{1}$$

where $P(\mathbf{x},\ t)$ is the pressure-time waveform of the acoustic pulse at the field point with space coordinates ($\mathbf{x} \equiv x,\ y,\ z$) and time $t$; $\mathbf{A}$ is a convolution-type operator describing absorption, $q \equiv P_0(B/A+2)/2\rho_0 c_0^2$ is the Mach number, $P_0$ is the source pressure amplitude; $\rho_0$, $c_0$, $B/A$ are the ambient density, sound velocity and nonlinearity parameter of the medium, respectively; $\beta \equiv B/2A+1$; $m \equiv f/f_0$ – dimensionless frequency; $f$ and $f_0$ – frequency and characteristic frequency; $a(m) = \alpha_1 \cdot m^b$ – parameter of absorption, $\alpha_1$ denotes small signal absorption coefficient at 1 MHz, $b$ is the power law of the attenuation frequency-dependence (for water $b = 2$, for soft tissues $b = 1$–$1.3$), $F^{-1}[\ldots]$ – the inverse Fourier transform.

If the propagation is linear (when in Eqs. (1) $q \equiv 0$) and $P^+(\mathbf{x},\ t)$ is the solution of the linear equation, the echoes from the positive pulses are the inversed copies of the echoes from the negative pulses, so the sum of echoes gives zero output $P^+(\mathbf{x},t) + P^-(\mathbf{x},t) = 0$.

Nonlinear propagation of two inverted pulses results in their distorted waveforms at any field point are not the inverse of each other, so their spectra are not the same. Then the spectrum of the sum of echoes from both the positive and negative pulses has the enhanced second harmonic components (being in phase) and the reduced fundamental ones (being in opposite phase).

Equations (2) and (3) describe the two initial waveforms with the opposite phase transmitted alternately for both the PI and MNC methods, respectively.

$$P_{\mathrm{PI}}(\mathbf{x},t) \equiv \left\{\begin{matrix} +\sin(\omega_1 t) \\ \text{or} \\ -\sin(\omega_1 t)\end{matrix}\right\} E(t) \Rightarrow \left\{\begin{matrix} P_p(\mathbf{x},t) \\ \\ P_n(\mathbf{x},t)\end{matrix}\right. \qquad \text{for} \quad \mathbf{x} \in S(\mathbf{x}), \tag{2}$$

$$P_{\mathrm{MNC}}(\mathbf{x},t) \equiv \left\{\begin{matrix} +\sin(\omega_1 t) \\ \text{or} \\ -\sin(\omega_1 t)\end{matrix} \quad + \quad \begin{matrix} +\sin(\omega_2 t) \\ \text{or} \\ -\sin(\omega_2 t)\end{matrix}\right\} E(t) \Rightarrow \left\{\begin{matrix} P_{pp}(\mathbf{x},t) \\ P_{pn}(\mathbf{x},t) \\ P_{np}(\mathbf{x},t) \\ P_{nn}(\mathbf{x},t)\end{matrix}\right. \qquad \text{for} \ \ \mathbf{x} \in S(\mathbf{x}). \tag{3}$$

Here $P_{\mathrm{PI}}(\mathbf{x}, t)$ and $P_{\mathrm{MNC}}(\mathbf{x}, t)$ are the initial pressure waveforms on the source surface for the PI and the MNC method, respectively; $E(t)$ is the pulse envelope function that is the same for both methods; $S(\mathbf{x})$ is the source surface; $\omega_1 = 2\pi f_1$, where $f_1$ is the fundamental frequency of both the single-tone (PI) and two-tone bursts (MNC); $\omega_2 = 2\pi f_2$, where $f_2 = 2f_1$ is the frequency of the second tone in two-tone bursts. It means that the transmitted two-tone bursts contain both the fundamental and second harmonic frequencies. Subscripts $p$ and $n$ indicate positive (+) and negative (−) polarization of tones, respectively.

In the PI method the pairs of single-tone bursts with the same envelope but opposite phases are transmitted alternately. The absolute values of their Fourier spectra are identical. Sum of both initial pulses is equal to zero. Due to nonlinearity of medium the initial sinusoidal pulses are distorted during propagation along the scan line. For field points that are not too close to the source surface the nonlinearly distorted positive and negative tone bursts have different waveforms and their spectra are also different. Thus, sum of received echoes is not equal to zero. Sum of their spectra enhance the second harmonic components and diminish the fundamental ones.

In the MNC method the operating principle is similar but involves two-tone bursts. Figure 1 shows four combinations of the initial two-tone bursts emitted in water and their spectra. All calculations have been done by means of the numerical solver recently developed by Wójcik *et al.* [11]. Numerical simulations of the nonlinear propagation of two-tone bursts in attenuating medium were performed

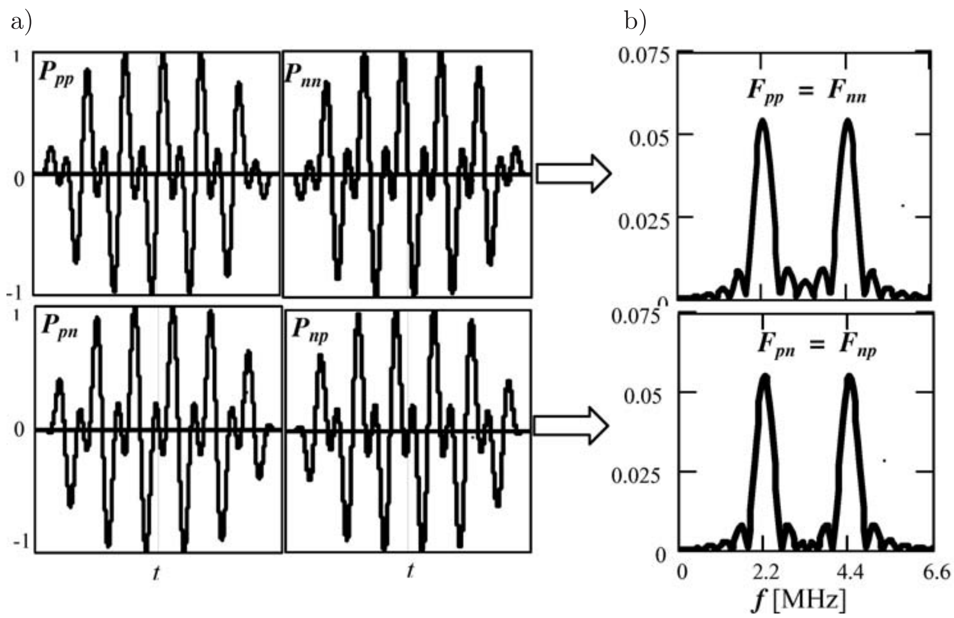


Fig. 1. Four configurations of the initial two-tone waveforms used in the MNC method (a) and the absolute values of their Fourier spectra (b).

for frequencies $f_1 = 2.2$ MHz, $f_2 = 4.4$ MHz. The following boundary conditions parameters were introduced to the numerical algorithm as the input data. The circular focused source parameters: diameter, $d = 12.8$ mm, focal length, $F = 40$ mm, source pressure amplitude, $P_0 = 0.5$ MPa. The acoustic parameters of medium (water): sound velocity, 1500 m/s, density, 1000 kg/m$^3$, absorption coefficient, $\alpha_1 = 2.5 \cdot 10^{-14}$ Np/(m·Hz$^2$), nonlinearity parameter, $(B/A)_w = 5$.

Although configurations of the initial two-tone pressure waveforms used in the MNC method are different the modules of their spectra is the same. Nonlinear effects accompanying propagation of the finite-amplitude acoustic wave in nonlinear attenuating medium results in the spectra of two-tone waveforms at some distance from the source are not the same. This is evident from Fig. 2 that shows the spectra of considered configurations in the focal plane.

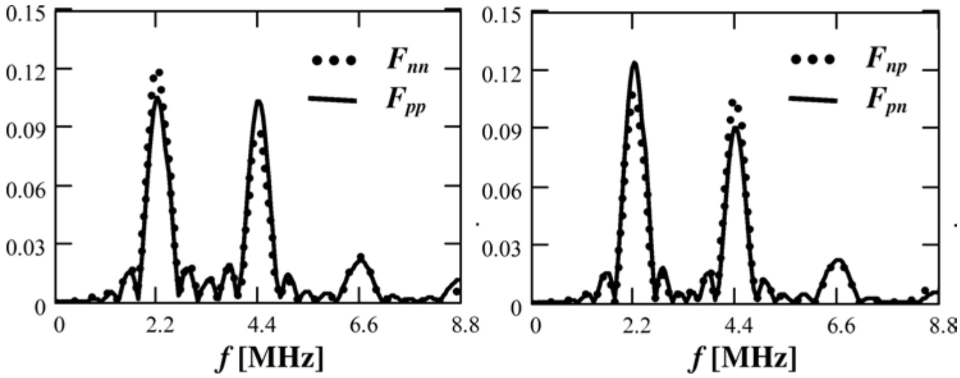


Fig. 2. Moduli of the Fourier spectra of four two-tone waveforms near the focal plane resulting in the nonlinear waveform distortion.

## 3. Combinations of two-tone bursts in the MNC method

The PI method involves transmitting along each scan line alternately two single-tone bursts of the same waveform but opposite in phase. Addition of the received echoes results in the summation of the nonlinearly generated second harmonic components that are approximately in phase. In this way the second harmonic of the sum waveform is enhanced and the fundamental is almost cancelled.

The MNC method involves transmitting along each scan line alternately two pulses being the combination of four configurations of the two-tone bursts mentioned. Six following combinations were considered:

$$\begin{aligned} P_{ppnn} &\equiv P_{pp} + P_{nn}, & P_{pnnp} &\equiv P_{pn} + P_{np}, \\ P_{pnnn} &\equiv P_{pn} + P_{nn}, & P_{pnnn} &\equiv P_{pn} + P_{nn}, \\ P_{pppn} &\equiv P_{pp} - P_{pn}, & P_{nnnp} &\equiv P_{nn} - P_{np}. \end{aligned} \tag{4}$$

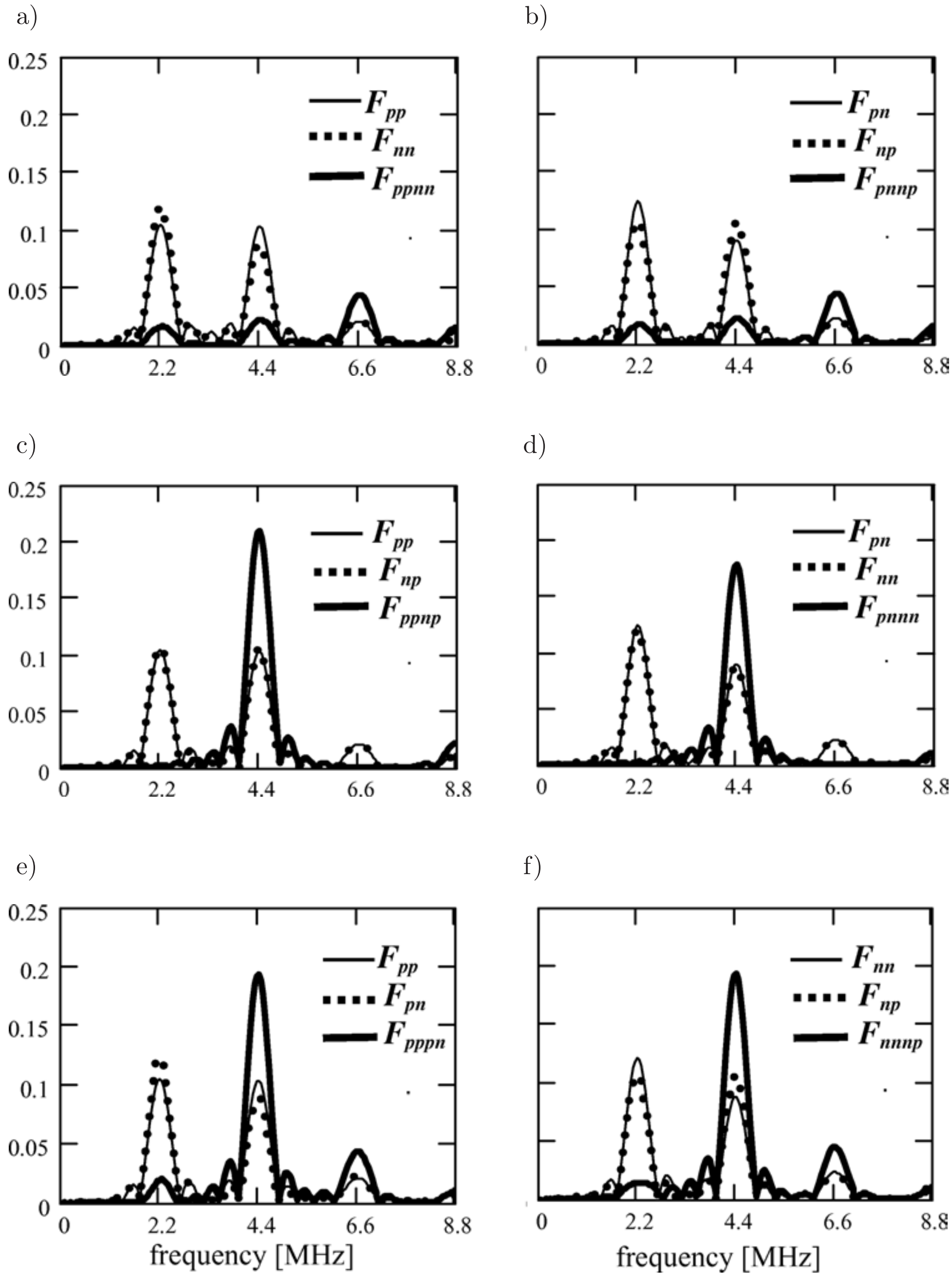


Fig. 3. Spectra for six combinations of the incident pulses used in the MNC method calculated in tissue on the beam axis near the focal plane. Cancellation of the spectral components at fundamental frequency is clearly visible (especially in (c) and (d) as well as generation of the third harmonics $f_3 = 6.6$ MHz (plots (a), (b), (e) and (f)).

As follows from Eqs. (4) received echoes are added or subtracted. The absolute value of the resulting spectra of sum or subtract signals in the focal area for the pulse propagating through tissue are shown in Fig. 3. This figure illustrates the examples of modules for spectra of pulses that compose the corresponding pairs. Both components of each pair were plotted in dotted and thin solid lines. The bold solid lines represent the modules of the resulting spectra. It should be taken into consideration that the two upper pairs of pulses in Eqs. (4) that produce combinations $P_{ppnn}$ and $P_{pnnp}$ (with spectra $F_{ppnn}$ and $F_{pnnp}$) comprise pulses with opposite polarization (that have opposite polarizations of component tones with respect to the polarization of tones in the second pulse within the pair). These two special cases of the MNC are referred as the multitone pulse inversion (MPI). In these two cases, as well as in cases illustrated in Figs. 3e and 3f, beside the second harmonic, the third harmonic $3f_1$ is generated. Under specific conditions, these higher harmonics can be also detected. It should be noted that for both the incident and backscattered fields the results, as defined in Eqs. (4), are not tangible physical objects that really exists. Rather they constitute virtual structures, as the fields that contribute to the formation of these objects do not coexist in the medium. The reason for introducing such objects will be explained in the next section.

## 4. Virtual fields

The concept of the virtual incident and backscattered fields helps to explain some properties (of side-lobes, signal-to-noise ratio, gain) and compare both the PI and MNC methods. Let us consider pulses $P_{pp}(t)$ and $P_{nn}(t)$, transmitted one after another along the scan line (Fig. 4a). Despite the difference of pulses in both the PI and MNC methods, the excitation and detection schemes are identical. Each has its own acoustical pressure field distribution. Considering the two subsequent pulses, they appear in time $t_1 \leq t \leq t_1 + t_T$ and $t_2 \leq t \leq t_2 + t_T$, respectively (where $t_1$ and $t_2$ are the start moments of the first and the second pulse, $t_T$ is the pulse duration). So, these pulses are not coexisting simultaneously in the medium and are not generating the real acoustical fields being their superposition.

However, the superposition of the individual pulses propagating separately can be easily processed by the computer. When both incident pulses are combined, the final virtual pulse is obtained (see Fig. 4C) and the corresponding spatial field distribution is called the incident virtual field. An example of the virtual intensity $I_{ppnn}(\mathbf{x})$ of the virtual incident field $P_{ppnn}(\mathbf{x}, t)$ for the two pulses $P_{pp}(\mathbf{x}, t)$ and $P_{nn}(\mathbf{x}, t)$ is shown in Fig. 4D.

The backscattered echoes $P^e_{pp}(t)$, $P^e_{nn}(t)$ are next combined and the resulting signal $P^e_{ppnn}(t)$ (Fig. 4E) can be considered an equivalent of the detected virtual backscattered field.

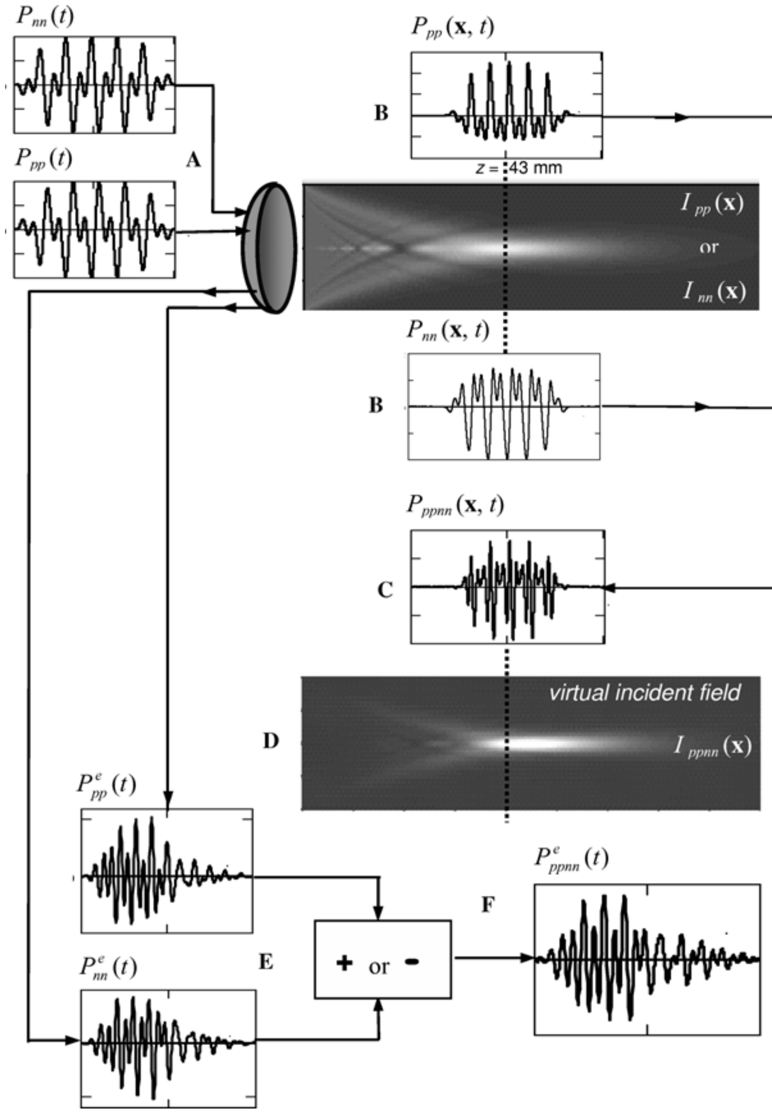


Fig. 4. Concept of the virtual fields. (A) The initial transmitted pulses $P_{nn}(t)$, $P_{pp}(t)$. (B) The nonlinearly distorted on-axis pressure waveforms $P_{nn}(\mathbf{x}, t)$, $P_{pp}(\mathbf{x}, t)$ in the focal plane $z$ = 43 mm and (C) their virtual sum $P_{ppnn}(\mathbf{x}, t)$. (D) The virtual intensity $I_{ppnn}(\mathbf{x}, t)$ for the sum pulse. (E) The echoes $P^e_{pp}(t)$, $P^e_{nn}(t)$ from the transmitted pulses and (F) their virtual sum $P^e_{ppnn}(t)$.

## 5. Properties of the original and virtual pulses in both the PI and MNC methods

Now let us discuss the properties of the incident original fields and virtual fields calculated for both the MNC and PI methods. The lateral resolution ability of both methods is compared in Fig. 5. In the upper-left corner the intensity field for one of the pulses $P_p$ transmitted in the PI method and for one pulse $P_{pp}$ out of four in the MNC are shown. The lateral beam width is plotted along the dashed white line and is narrower than that when two-tone bursts are transmitted. The right middle and bottom beams width plots help to compare the normalized intensities of virtual fields for the PI method with two different combinations of pulses ($P_{ppnn} \equiv P_{pp} + P_{nn}$ and $P_{nnnp} \equiv P_{nn} - P_{np}$) in the MNC method. For the both cases "two-tone" beams are narrower than that obtained by the PI method.

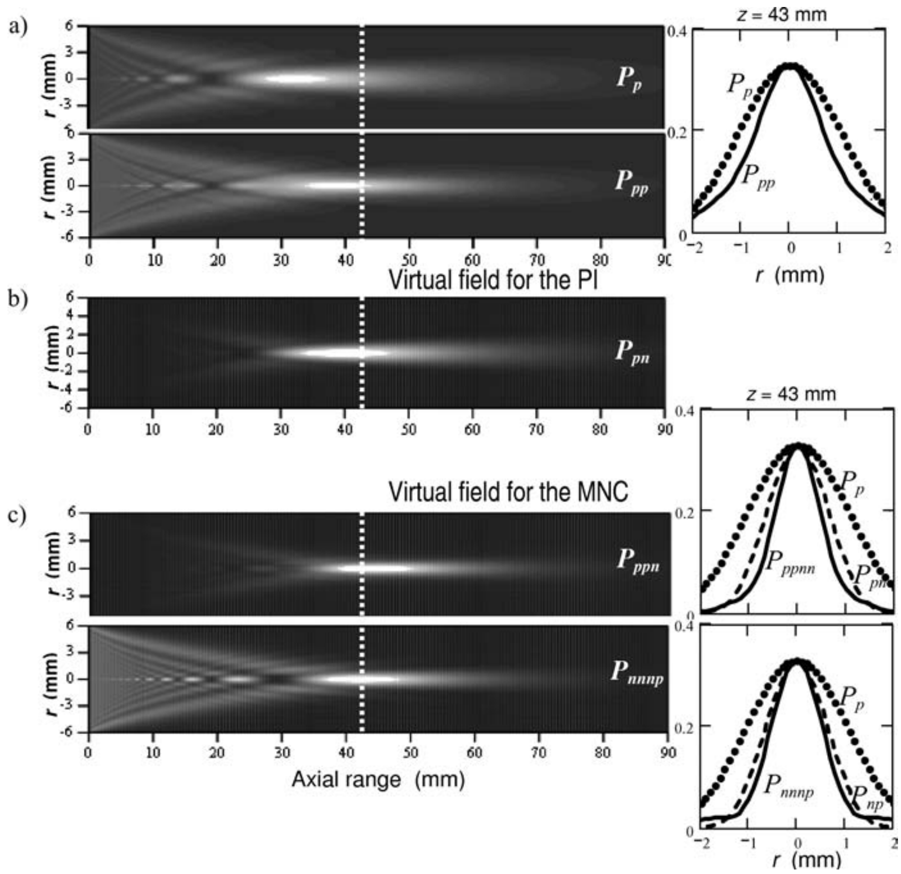


Fig. 5. Intensity distributions (left) along the beam in the $(r, z)$ plane and lateral pressure distributions (right) in the focal range ($z = 43$ mm) for fields produced (a) by positive single-tone $P_p$ (dotted lines) and two-tone $P_{pp}$ pulses as well as for virtual fields generated (b) by the sum $P_{pn}$ of positive $P_p$ and negative $P_n$ pulses in the PI method (dashed lines) and (c) by the combinations of the two-tone pulses $P_{ppnn}$ and $P_{nnnp}$ in the MNC method (solid lines).

In order to compare the MNC method developed with the PI method three different parameters were calculated for both of them, these were the mechanical index (MI), the energy (E) and the lateral resolution measured as a full-width of the beam at half-maximum pressure (FWHM). The same envelope, pulse duration and peak-pressure ($P_0 = 0.5$ MPa) on the transducer surface were assumed for both the single-tone (2.2 MHz) and two-tone (2.2 MHz + 4.4 MHz) bursts. Naturally, the MI for two-tone transmission is lower due to the average frequency diminishes for the pulse being a sum of two-tone sinusoidal pulses of the same duration but differing in frequency by a factor of two. The ratio of energies and beam-widths are also in favor of the multi-tone transmission and the actual values are as follows:

$$\frac{\mathrm{MI}_{\mathrm{PI}}}{\mathrm{MI}_{\mathrm{MNC}}} = \frac{0.789}{0.56} \cong 1.41, \qquad \frac{I_{\mathrm{PI}}(\mathbf{x})}{I_{\mathrm{MNC}}(\mathbf{x})} > \frac{\mathrm{E}_{\mathrm{PI}}}{\mathrm{E}_{\mathrm{MNC}}} = 1.65.$$

It should be noticed that MI for the PI method is by more than 40% higher than for the MNC method. The slight improvement in lateral resolution with respect to the PI method is also noticed:

$$\frac{\mathrm{FWHM}_{\mathrm{MNC}}}{\mathrm{FWHM}_{\mathrm{PI}}} \approx 1.3.$$

The ratios of intensities, calculated for virtual fields for two cases of the MPI (Multitone Pulse Inversion) method and other cases as well as the ratio of the corresponding FWHM beam widths are equal to

$$\frac{I_{\mathrm{MPI}}}{I_{\mathrm{PI}}} \cong 0.63, \qquad \frac{I_{\mathrm{MNC}}}{I_{\mathrm{PI}}} \cong 6, \qquad \frac{\mathrm{FWHM}_{\mathrm{MNC}}}{\mathrm{FWHM}_{\mathrm{PI}}} \cong 1.1\text{–}1.3.$$

The first ratio stands for the decrease of the virtual energy, the second one shows that the virtual energy increases. The increase of the ratio of the virtual field intensities indicates the advantage of the new method: the gain in echoes is reached without any additional thermo-mechanical effects.

## 6. Discussion

In conventional tissue harmonic imaging (THI) a single-tone burst is applied to the acoustic source and then the second harmonics echo is extracted to produce tissues images with presumably improved resolution. However, as it was mentioned before, the transducer transmitting/receiving bandwidth and efficiency are used in insufficient way, as only half of the bandwidth is occupied during transmission. This is the case for both the standard harmonic imaging and PI techniques. In the novel multi-tone coding (here two harmonic tones are considered) full available bandwidth is employed during transmission and reception.

Consequently, for the MNC method the acoustic energy available for image construction can be even two-fold larger, with the corresponding increase in signal-to-noise ratio compared to the conventional harmonic imaging. In the description of the phenomena accompanying propagation of signals used in the harmonic imaging PI and MNC methods the second order nonlinear partial differential equation describing the model in a dimensionless system of units have been solved (Wójcik 1998).

All results presented in this paper were computed using the previously developed numerical algorithm solving Eqs. (1). The following boundary conditions parameters were assumed: spherical focused transducer with a diameter of 12.8 mm and focal length of 60 mm. The media examined had the absorption coefficient equal to $\alpha_1 = 7$ Np/(m·MHz) and the nonlinearity parameter $B/A = 5$. The peak pressure amplitude on the transducer surface was assumed to be $P_0 = 0.5$ MPa.

The advantages of the MNC method developed with respect to the PI method are:

- Mechanical Index for the MNC method is lower in comparison to the PI method for the same initial peak-to-peak pressure ($\mathrm{MI_{PI}}/\mathrm{MI_{MNC}} = (0.789/0.56) \approx 1.4$;
- Lateral resolution is better for the MNC method with respect to the PI method by a factor of 1.1–1.3;
- Compared with the PI method the new approach allows to process six different decoding schemes of the received echoes (two out of six correspond to the MPI).

In the media with strong absorption, the pressure amplitude ratio of the MNC/PI was between 0.5 and 1 for signals $P_{ppnn}$ and $P_{pnnp}$ (called the MPI). For other four cases this ratio was between 6 and 8. It should be noted that the signal gain for the MNC method diminishes with decreasing absorption of the medium examined. For water this ratio was equal to 1 and 2 respectively.

Depending on the processing scheme, the different spectral components of the resulting spectra can be enhanced. This can result in the optimal compensation or rejection of the fundamental component, leaving the only second harmonic or even transferring part of the received energy to the higher harmonics.

## Acknowledgments

This work has been supported by the Ministry of Science and Higher Education of Poland from means on science in 2007–2010 (research project No. 518 002 32/0219).

## References

[1] Averkiou M.A., Roundhill D.R., Powers J.E., *A new imaging technique based on the nonlinear properties of tissues*, Proc. IEEE Ultrason. Symp., **2**, 1561–1566 (1997).

[2] Averkiou M.A., *Tissue Harmonic Ultrasonic Imaging*, CR Acad. Sci., **2**, 1139–1151 (2001).

[3] Becher H., Tiemann K., Pohl C., Nanda N., Averkiou M.A., Powers J.E., Luderitz B., *Improvement in endocardial border delineation using tissue harmonic imaging*, Echocardiography, **15**, 511–517 (1998).

[4] Tranquart F., Grenier N., Eder V., Pourcelot L., *Clinical use of ultrasound tissue harmonic imaging*, Ultrasound in Med. & Biol., **25**, 6, 889–894 (1999).

[5] Christopher T., *Finie amplitude distortion-based inhomogeneous pulse echo ultrasonic imaging*, IEEE Trans. UFFC, **44**, 1, 125–139 (1997).

[6] Christopher T., *Experimental investigation of finite amplitude distortion-based second harmonic pulse echo ultrasonic imaging*, IEEE Trans. UFFC, **45**, 1, 158–162 (1998).

[7] Gong X., Ye S., Zhang D., *Measurement of nonlinearity parameter of contrast agents* [in:] Nonlinear acoustics in perspective, Wei R.J. [Ed.], Nanjing University Press, Nanjing China, 475–480 (1996).

[8] Wu J., Tong J., *Measurements of the nonlinearity parameter B/A of contrast agents*, Ultrasound in Med. & Biol., **24**, 1, 153–159 (1998).

[9] Simpson Hope D., Chin C.T., Burns P.N., *Pulse inversion Doppler: a new method for detecting nonlinear echoes from micro-bubble contrast agents*, IEEE-UFFC Trans., **6**, 2, 372–382, 1999.

[10] Wójcik J., *Nonlinear reflection and transmission of plane acoustics waves*, Archives of Acoustics, **29**, 4, 607–632, 2004.

[11] Wójcik J., Nowicki A., Lewin P.A., Bloomfield P.E., Kujawska T., Filipczyński L., *Wave envelopes method for description of nonlinear acoustic wave propagation*, Ultrasonics, **44**, 310–329, 2006.